Journal of Solid State Chemistry 184 (2011) 2794–2798

Contents lists available at SciVerse ScienceDirect

Journal of Solid State Chemistry

journal homepage: www.elsevier.com/locate/jssc

Crystal and electronic structure study of $AgPd_3Se$

F. Laufek [a,*], A. Vymazalová [a], D.A. Chareev [b], A.V. Kristavchuk [b], Q. Lin [c], J. Drahokoupil [d], T.M. Vasilchikova [e]

[a] Czech Geological Survey, Geologická 6, 152 00 Praha 5, Czech Republic
[b] Institute of Experimental Mineralogy RAS, Chernogolovka, Russia
[c] Department of Chemistry, Iowa State University, Ames, IA 50011, USA
[d] Institute of Physics, ASCR v.v.i., Na Slovance 2, 182 21 Prague 8, Czech Republic
[e] Moscow State University, Department of Physics, Moscow 119991, Russia

ARTICLE INFO

Article history:
Received 26 May 2011
Received in revised form
9 August 2011
Accepted 14 August 2011
Available online 23 August 2011

Keywords:
$AgPd_3Se$
Crystal structure
Selenides
Friauf polyhedra
Quasicrystal

ABSTRACT

The $AgPd_3Se$ compound was synthesised from individual elements by solid-state chemical reactions and structurally characterized by powder X-ray diffraction data. $AgPd_3Se$ displays cubic symmetry, space group $Pa\bar{3}$, unit cell parameter $a=8.6289(1)$ Å and $Z=8$. Double-Friauf polyhedra (DFP), defined by Pd and Se atoms, form the basic structural building block of the $AgPd_3Se$ crystal structure. The Ag atoms occupy the centres of DFPs forming an Ag–Ag dimer (2.792(2) Å). The packing of DFPs forms two kinds of interpenetrating networks that show similar features as three-dimensional Penrose tiles. $AgPd_3Se$ is isostructural with $CaAu_3Ga$. The electric resistivity as well as the electronic structure calculation suggests metallic behaviour.

1. Introduction

During the investigation of phase relations in the Pd–Ag–Se system, a new phase $AgPd_3Se$ was discovered. Among ternary Pd–Ag selenides, the examples encountered so far are Pd_2Ag_2Se [1] and $Ag_2Pd_3Se_4$ [2]. Up to now, only the crystal structure of the $Ag_2Pd_3Se_4$ phase, which is also known as a mineral chrisstanleyite, is determined. This is surprising because numerous structural studies have been devoted to the binary palladium and silver selenides (summarised in Ref. [3]). These metal-rich chalcogenides have also attracted a great deal of attention during last decades mainly because of their interesting structural chemistry and unusual physical properties, which put this class of compounds at the interface of chemistry, mineralogy, solid state physics and materials science [4–7].

In this paper, we present synthesis, crystal structure and electronic structure calculation of new ternary compound $AgPd_3Se$. The resistivity measurements are also reported. Preliminary structural data about title phase were presented in a conference abstract [8].

2. Experimental

2.1. Synthesis and chemical composition

The ternary compound $AgPd_3Se$ was prepared by high-temperature solid-state reactions. Stoichiometric amounts of silver (99.999%), palladium (99.95%) and selenium (99.999%) were loaded into the high-purity silica glass tube and tightly fitting silica glass rod was placed on the top of the reagents in order to keep the charge in place and also to reduce the vapour volume on heating. The evacuated tube with its charge was at first annealed at 800 °C for 2 days. After regrinding in acetone, the sample was again heated at 350 °C for 62 days. The temperature was controlled electronically (± 4 °C). After heating, the sample was quenched in a cold-water bath.

Chemical analyses were carried out on a Cameca SX-100 electron microprobe using the wave-length-dispersion mode and a focused beam (size 1–2 μm). The accelerating voltage was set to 15 kV and the beam current was 10 nA. The samples were analysed using PdL_α, AgL_β and SeL_α. Pure metals (Pd, Ag and Se) were used as primary standards. Data were collected (five readings) from different spots on several different crystals and than averaged. The chemical analysis of the specimen used for the crystal structure analysis yielded an overall composition of $Ag_{1.00(2)}Pd_{3.04(2)}Se_{0.96(1)}$ (based on five atoms per formula unit).

* Corresponding author. Fax: +420 251 818 748.
E-mail address: frantisek.laufek@geology.cz (F. Laufek).

0022-4596/$ - see front matter © 2011 Elsevier Inc. All rights reserved.
doi:10.1016/j.jssc.2011.08.019

2.2. Crystal structure determination and refinement

The powder X-ray diffraction pattern used for the structure determination was collected in Bragg–Brentano geometry on an X'Pert Pro PANalytical diffractometer, equipped with an X'Celerator detector using Co$K\alpha$ radiation. To minimize background, the sample was placed on a flat low-background silicon wafer. The data were collected in the range from 12 to 160° 2θ. A full-width at half maximum of 0.099° 2θ was obtained at 40.217° 2θ indicating a good crystallinity of the studied sample. The details of the data collection and basic crystallographic facts are given in Table 1.

The indexing of the X-ray powder pattern was performed using the DICLVOL06 program [9]. The first 20 lines, with an absolute error of 0.03° 2θ on peak positions, were indexed on the basis of the cubic cell listed in Table 1. The figures of merit M_{20} [10] and F_{20} [11] for assessing the quality of the solution were $M_{20}=336$ and $F_{20}=231$ (0.0018, 49), respectively.

The extraction of the integral intensities as well as the structure solution by direct methods was accomplished using the EXPO2004 program [12]. The structure was solved in space groups consistent with systematic absences ($P4_232$, $P4_132$, $P2_13$, $Pa\bar{3}$), however only the solution in the $Pa\bar{3}$ space group resulted in physically sensible geometry. Three crystallographic positions were found; one of them was assigned as Se position (8*c*), two of them temporary as Pd positions (24*d* and 8*c*).

The structural model found by EXPO2004 was introduced into the FullProf program [13] for Rietveld refinements. A pseudo-Voigt function was selected to describe individual line profiles; the background was determined by the linear interpolation between consecutive breakpoints in the pattern. Intensities within 15 times the full width at half maximum of a peak were considered to contribute to the central reflection. Because it is nearly impossible to distinguish the Ag and Pd atoms using conventional powder X-ray diffraction, the measured chemical composition of the sample – $Ag_{1.00(2)}Pd_{3.04(2)}Se_{0.96(1)}$ – was also used to designate the Ag position. According to the electron microprobe analyses, the ratio of Ag, Pd and Se compositions was determined to be very close to 1:3:1, which happens to correspond to the ratio of the multiplicities of the three Wyckoff positions (8*c*, 24*d* and 8*c*) obtained in the initial crystal structure solution. Hence, the position at the 8*c* site, temporarily assigned as Pd, was changed to the Ag position in later refinements. Nevertheless, the possibility that a certain degree of mixing of the Pd and Ag atoms occurs on their two sites cannot be ruled out. Rietveld refinements with Pd/Ag (24*d*) and Ag/Pd (8*c*) mix sites do not reveal any significant change in displacement or profile agreement parameters. However, both elements are essential for structure formation, because no structural analogues were found in the corresponding binary systems Pd–Se and Ag–Se.

The final refinement with all 18 parameters, including 7 profile, 5 positional and 3 isotropic displacement parameters converged to $R_{Bragg}=0.036$ and $R_{wp}=0.027$. The chemical composition $Ag_{1.00(2)}Pd_{3.04(2)}Se_{0.96(1)}$ obtained from electron microprobe is very close to the final crystal structure refinement of $Ag_{1.00}Pd_{3.00}Se_{1.00}$. The details of the refinements are summarised in Table 1, the refined atomic coordinates and isotropic displacement parameters are listed in Table 2. The experimental (red circle), the calculated (black curve), the peak positions (green bar), and the difference curves (blue) after the final Rietveld refinement are shown in Fig. 1.

2.3. Electronic structure calculation

The densities-of-states (DOS) were calculated by means of the self-consistent, tight-binding, linear-muffin-tin-orbital (LMTO) methods in the local density (LDA) and atomic sphere (ASA) approximations, within the framework of the DFT method [14–17]. ASA radii for atomic sites were scaled at the limitation of 16% maximum overlap between two neighbouring atomic spheres, and interstitial spheres were introduced accordingly. The ASA radii for Pd, Ag and Se were 2.65 Å, 3.09 Å and 2.79 Å, respectively. Reciprocal space integrations were carried out by means of the tetrahedron method. The basis sets were 5*s*/5*p*/4*d*/(4*f*) for Pd, 5*s*/5*p*/4*d*/(4*f*) for Ag, and 4*s*/4*p*/(4*d*) for Se, with orbitals in parentheses down-folded [18]. Scalar relativistic effects were automatically included in the calculations. The band structure was sampled for $24\times24\times24$ *k* points in the irreducible wedge of the Brillouin zone. The crystal orbital Hamilton population

Table 1
Data collection and Rietveld analysis. *R* agreement factors defined according to Ref. [26].

Data collection	
Radiation type, source	X-ray, Co$K\alpha$
Generator settings	40 kV, 30 mA
Data collection temperature	room temperature
Range in 2θ (deg.)	12–160
Step size (deg.)	0.033
Crystal data	
Space group	$Pa\bar{3}$(No. 205)
Unit cell content[a]	$Ag_{1.00(2)}Pd_{3.04(2)}Se_{0.96(1)}$, $Z=8$
Unit cell parameters (Å)	$a=8.6289(1)$
Rietveld analysis	
No. of reflections	154
No. of structural parameters	8
No. of profile parameters	6
R_{Bragg}	0.036
R_p	0.021
R_{wp}	0.027
Weighting scheme	$1/y_o$

[a] According to the electron microprobe analysis.

Table 2
Refined atomic coordinates for the $AgPd_3Se$.

Atom	Site	*x*	*y*	*z*	B_{iso} [Å^2]
Pd(1)	24*d*	0.5869(1)	0.2227(1)	0.6377(1)	0.46(3)
Ag(1)	8*c*	0.4066(1)	0.4066(1)	0.4066(1)	0.59(4)
Se(1)	8*c*	0.1230(2)	0.1230(2)	0.1230(2)	0.31(7)

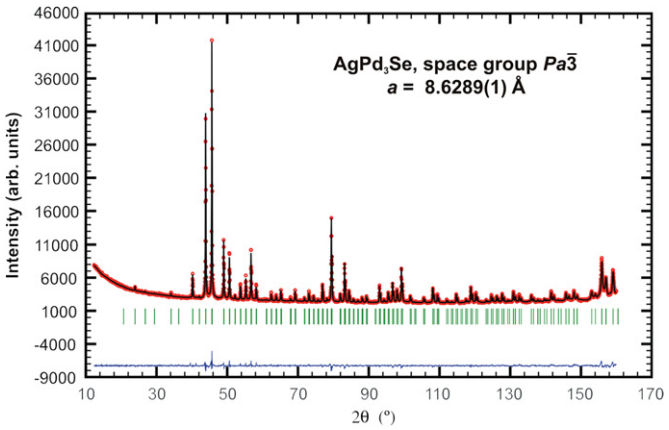

Fig. 1. Observed (circles), calculated (solid line) and difference Rietveld profiles for $AgPd_3Se$. The vertical bars indicate the positions of the Bragg peaks. (For interpretation of the references to colour in this figure, the reader is referred to the web version of this article.)

(COHP) analyses were also performed to gain insight into the bonding properties [19].

2.4. Electrical resistivity

The electrical resistivity measurements were carried out using the four-probe method: two contacts were adjusted on the edges of the sample and two in the centre. Contacts were sealed with tin. The powder sample was pressed (under the weight of 2 t) into the shape of parallelepiped with dimensions $2 \times 3 \times 8$ mm^3. The electrical resistance was studied in the range from room temperature up to the temperature of liquid nitrogen, in heating and cooling cycles.

3. Results and discussion

3.1. Crystal structure

The crystal structure of $AgPd_3Se$ is isostructural with $CaAu_3Ga$ [20]. Similar motifs were also observed in the structures of $NaAu_3Si$ and $NaAu_3Ge$ [21]. In the structure of $AgPd_3Se$, each Ag atom is surrounded by 12 Pd, 3 Se and 1 Ag atoms, as is indicated in Fig. 2(a). Twelve of these atoms (9Pd and 3Se) form a distorted truncated tetrahedron, also known as Friauf polyhedron. The Friauf polyhedron is one of the most common coordination polyhedra in intermetallic phases and Frank–Kasper type quasicrystals [22]. As shown in Fig. 2(b), two adjacent Friauf polyhedra share a common hexagonal face, composed of Pd atoms, forming a double Friauf polyhedron (DFP). The DFP forms the basic structural building block of the $AgPd_3Se$ crystal structure. The central Ag atoms form an Ag–Ag dimer (2.792(2) Å) that is oriented across the shared hexagonal face. More specifically, the Ag–Ag dimer lies in the threefold axis of the DFP. The packing of DFPs in the $AgPd_3Se$ crystal structure cannot fill all the space without gaps, as was mentioned by Lin and Corbett [20] for the isostructural $CaAu_3Ga$. These gaps, each defined by three Pd and one Se atoms, are exactly the parts that are truncated along the threefold axis of the Friauf polyhedron. As shown in Fig. 2(c), each DFP shares its Pd_3 face with two neighboring Pd_3Se tetrahedral voids to form a more complex structural unit, namely prolate rhombohedron (PR). The decoration of the PR is prominent: the electron-rich Se atoms always occupy the vertices, whereas the electron-poor Pd atoms are located approximately to the midpoints of the Se–Se edges (Fig. 3). Similar "colouring" is seen in $CaAu_3Ga$ [20], $NaAu_3Si$ and $NaAu_3Ge$ [21]. All Se–Se edges of the PR show the same length of 4.827(2) Å, which is approximately close to the sum (4.904 Å) of two individual Pd–Se distances of 2.475(2) Å and 2.429(2) Å. Compared with the Ga-based PR in $CaAu_3Ga$ [20], the Se-PR are more distorted; the Se–Pd–Se and Ga–Au–Ga angles are 161.06(6)° and 172.08(5)°, respectively.

Similar to the Ca network in $CaAu_3Ga$ [20], the interconnection of eight Ag atoms in each unit cell $AgPd_3Se$ forms an oblate rhombohedron (OR), or a squeezed cube along a threefold axis. The short diagonal (2.792(2) Å) of the OR overlaps with the unique threefold axis of the Se–PR (see Fig. 3). The Ag–Ag edges of OR are slightly longer than that of the Se–PR (5.090(2) Å vs. 4.827(2) Å). Noteworthy is that although Ag is about 0.09 Å larger than Ga in metallic radii (r_{Ga}=1.35 Å, r_{Ag}=1.44 Å, [23]), the Ag–Ag edge is shorter than the corresponding Ga–Ga edge (5.245(4) Å) observed in the $CaAu_3Ga$ structure [20]. The reason is because the PR and OR in the title structure are more distorted than those in $CaAu_3Ga$ (as discussed above).

Consequently, the $AgPd_3Se$ crystal structure can be viewed as a combination of two kinds of three-dimensional networks composed of Pd, Se (Fig. 4(a)) and Ag atoms (Fig. 4(b)), respectively. Their mutual interpenetration is shown in Fig. 4(c). This arrangement was described in detail in the structure of $CaAu_3Ga$ [20], therefore we will not review it thoroughly here. Nevertheless, it is interesting to note that the packing of PRs automatically generate

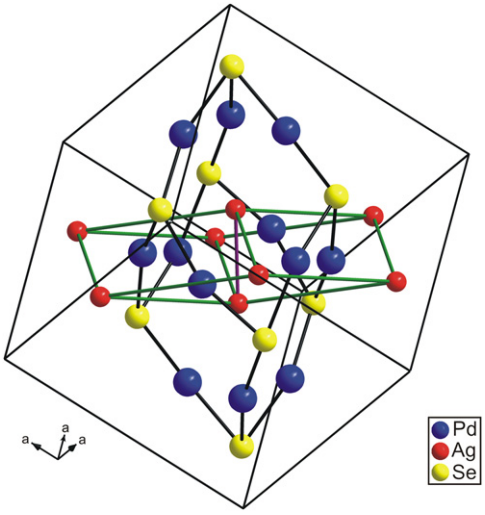

Fig. 3. Prolate (black lines) and oblate (green lines) rhombohedra in the unit cell of $AgPd_3Se$. The Ag–Ag dimer is highlighted (violet line). (For interpretation of the references to colour in this figure legend, the reader is referred to the web version of this article.)

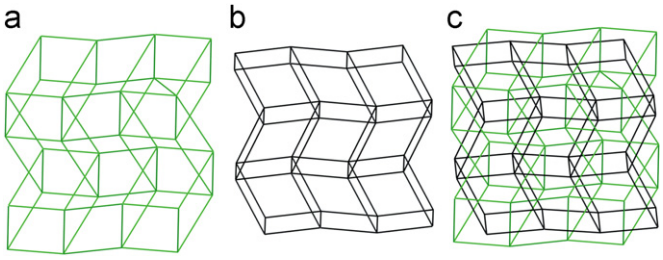

Fig. 4. The 3D networks of (a) Se atoms and (b) Ag atoms in the crystal structure of $AgPd_3Se$. The packing of Se prolate rhombohedra automatically generates its duals, Se oblate rhombohedra and vice versa. The same is valid for packing of Ag oblate rhombohedra. (c) The interpenetration of both networks.

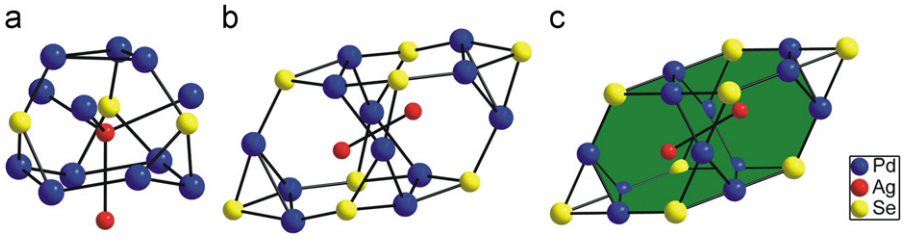

Fig. 2. (a) Coordination of the Ag atoms in the $AgPd_3Se$ crystal structure where 12 atoms (9Pd+3Se) form the truncated tetrahedron. (b) Two truncated tetrahedrons sharing a face forming a double Friauf polyhedron (DFP), the Ag–Ag dimer is emphasized. (c) An idealized drawing of the DFP.

their duals—ORs and vice versa. Moreover, PR and OR are the two basic units of the three-dimensional Penrose tiles (3DPTs) [24] that have been proved useful for quasicrystals modelling [25]. The acute Ag–Ag–Ag angle in the OR is 63.26(2)° in the $AgPd_3Se$ crystal structure, which is very close to the characteristic angle of 63.43° of the ideal 3DPTs. However, the acute Se–Se–Se angle, 66.22(3)° shows much larger deviation from the ideal geometry of 3DPTs.

Noteworthy is that in structures of $CaAu_3Ga$, $NaAu_3Si$ and $NaAu_3Ge$, the most electropositive elements Ca or Na occupy the centers of double Friauf polyhedra (DFPs), whereas the most electronegative Au, midpoints of PR edges, and the remaining triel (Ga) or tetrels (Si, Ge), the vertices. In the structure of $AgPd_3Se$, centers of DPFs remain being occupied by the most electropositive Ag (4.44 eV); however, the vertices are occupied by the most electronegative Se (5.89 eV) rather than Pd (4.45 eV). The reason must relate to the strong relativistic effect of Au, which results a large electron affinity. Actually in this structural type, the electronic structure of Pd is closer to that of Au than Ag (below).

3.2. Electronic structure

Fig. 5 shows (a) the densities-of-states (DOS) and (b) the crystal Hamilton overlap population (–COHP) data of $AgPd_3Se$. In the DOS patterns, the Fermi level (E_F) locates in a pseudogap, indicating a metallic character. The metallic character of $AgPd_3Se$ was also supported by the relatively low value of resistivity ($3.55\times10^{-4}\,\Omega$ cm at 300 K) and its temperature dependence (Fig. 6). The resistivity decreases as temperature decreases, which is typical for a metal. Interestingly, open gap is observed in M→X→G→R directions in the Brillouin zone at about 0.5 eV (Fig. 7), with only a band crossing from G→M direction. As shown in Fig. 5(a), the states far below E_F are mainly the Se 4*s* states, which are well separated from its 4*p* states because of its inert lone pair character. Heavy mixings of different states are observed in the energy range of ~−7.0 eV and up. The Pd 4*d* states spread in a large energy range, from ~−5.0 to E_F, similar to those of Au in $CaAu_3Ga$ and other Au-rich polar intermetallics. On the contrary,

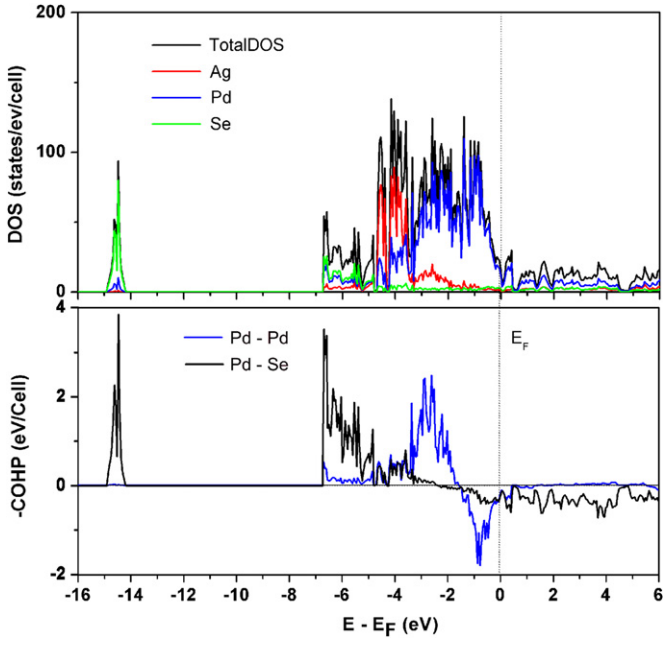

Fig. 5. (a) The densities-of-states (DOS) and (b) the crystal Hamilton overlap population (–COHP) data for $AgPd_3Se$.

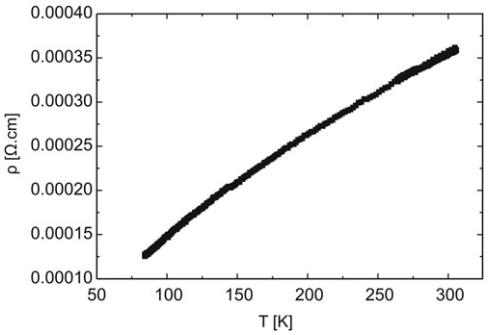

Fig. 6. Temperature dependence of the resistivity of $AgPd_3Se$.

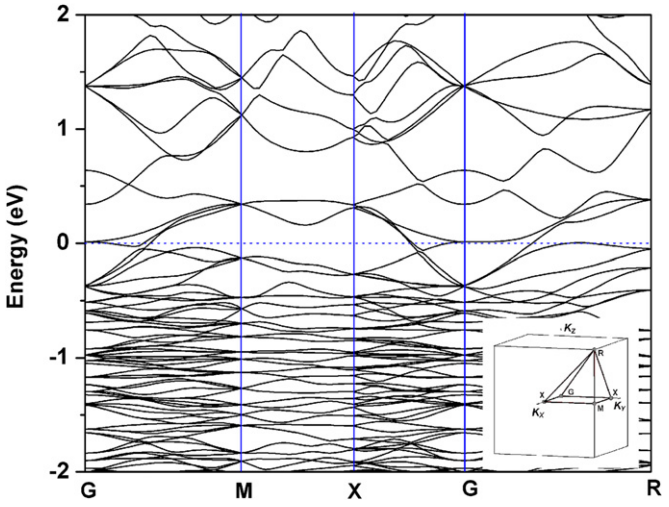

Fig. 7. The band structure for $AgPd_3Se$.

the 4*d* states of the Ag are much more localized within −5.0 eV to −3.0 eV. This supports the structural refinement results that Pd in $AgPd_3Se$ taking the Au positions in $CaAu_3Ga$. The most different electronic features between $CaAu_3Ga$ and $AgPd_3Se$ are the contributions of *d* states of the relative more electropositive Ca and Ag. In $CaAu_3Ga$, the Ca 3*d* states mainly populate above E_F but with some run across E_F to the valence band. However, the contribution of Ag 4*d* state around E_F in $AgPd_3Se$ is negligible (Fig. 5); rather, some Pd 4*d* states spread to the conduction band region, behaving as the Ca 3*d* in $CaAu_3Ga$.

According to the –COHP data, Fig. 5(b), the bonds within the anionic network (Pd–Pd and Pd–Se) exhibit small anti-bonding character at E_F, whereas the other Ag–Se, Ag–Ag, and Ag–Pd bonds are completely optimized (not shown). However, all these bonds are better optimized at ~0.5 eV, where 4 additional bands (or 8 electrons) would be required under rigid band assumptions. The band structure also supports this idea. As shown in Fig. 7, small pockets around E_F are observed, suggesting that small number of electrons or holes will not result in a change of the structure. Since these additional bands are mainly Pd 4*d* character, chemical tunings for semiconductors by partial replacements of Pd with electron-richer transition metals might be interesting.

4. Conclusions

To conclude, the new ternary compound $AgPd_3Se$ was structurally characterized. The basic structural building block of this phase is a double-Friauf polyhedron (DFP) composed of Pd and Se

atoms, which is centered by Ag atoms. The packing of DFPs forms two kinds of interpenetrating networks that show similar features as three-dimensional Penrose tiles.

The measurement of electrical resistivity and electronic structure calculation reveal metallic behavior of $AgPd_3Se$.

Acknowledgment

This research is funded through the project LA 11125/KONTAKT II from the Ministry of Education, Youth and Sports of the Czech Republic, and supported by a grant of the President of the Russian Federation for State Support of Young Russian Scientists (MK-1557.2011.5).

References

[1] A. Vymazalová, M. Drábek, F. Laufek, D.A. Chareev, A.V. Kristavchuk, M.V. Voronin, E.G. Osadchii, Acta Mineral. Petrogr. (2010) Abstract series, CD-ROM.
[2] D. Topa, E. Makovicky, T. Balič-Žunič, Can. Mineral 44 (2006) 497.
[3] E. Makovicky, in: D. J. Vaughan (Ed.). Sulfide Mineralogy and Geochemistry, Reviews in Mineralogy and Geochemistry, vol. 61, Mineralogical Society of America, Virginia, USA, pp. 7–107.
[4] A. Simon, in: A.K. Cheetham, P. Day (Eds.), Solid State Chemistry Compounds, Oxford University Press, Oxford, 1992, pp. 112–165.
[5] W. Tremel, H. Kleinke, V. Derstroff, C. Reisner, J. Alloys Compd. 219 (1995) 73–82.
[6] R. Pocha, C. Löhnert, D. Johrendt, J. Solid State Chem. 180 (2007) 191.
[7] D. Bichler, R. Pocha, C. Löhnert, Z. Anorg. Allg. Chem. 635 (2009) 48.
[8] F. Laufek, A. Vymazalová, M. Drábek, J. Drahokoupil, D.A. Chareev, A.V. Kristavchuk, Mater. Struct. 17 (2010) 76.
[9] A. Boultif, D. Louër, J. Appl. Cryst. 37 (2004) 724.
[10] P.M. de Wolff, J. Appl. Cryst. 1 (1968) 108.
[11] G.S. Smith, R.L. Snyder, J. Appl. Cryst. 12 (1976) 60.
[12] A. Altomare, R. Caliandro, M. Camalli, C. Cuocci, C. Giacovazzo, A. Moliterni, R. Rizzi, J. Appl. Cryst. 37 (2004) 1025.
[13] J. Rodríguez-Carvajal, FullProf.2k Rietveld Profile Matching & Integrated Intensities Refinement of X-ray and/or Neutron Data (powder and/or single-crystal), Laboratoire Léon Brillouin, Centre d'Etudes de Saclay, Gif-sur-Yvette Cedex, France, 2006.
[14] R. Tank, O. Jepsen, A. Burkhardt, O.K. Andersen, TB-LMTO-ASA Program, Vers. 4.7, Max-Planck-Institut für Festkörperforschung, Stuttgart, Germany, 1994.
[15] H.L. Shriver, The LMTO Method, Springer-Verlag, Berlin, Germany, 1984.
[16] O. Jepsen, M. Snob, Linearized Band Structure Methods in Electronic Band-Structure and its Applications, Springer Lecture Notes, Springer Verlag, Berlin, Germany, 1987.
[17] O.K. Anderson, O. Jepsen, Phys. Rev. Lett. 53 (1984) 2571.
[18] W.R.L. Lambrecht, O.K. Andersen, Phys. Rev. B34 (1986) 2439.
[19] R. Dronskowski, P. Blöch, J. Phys. Chem. 97 (1993) 8617.
[20] Q. Lin, J.D. Corbett, Inorg. Chem. 47 (2008) 3462.
[21] W. Doering, H.U. Schuster, Z. Naturforschung. B35 (1980) 1482.
[22] S. Francoual., M. deBoissieu, R. Currat, K. Shibata, Y. Sidis, B. Hennion, A.P. Tsai, J. Non-Cryst. Solids 353 (2007) 3182.
[23] N.N. Greenwood, A. Earnshaw, Chemistry of the Elements, second ed., Butterworth-Heinemann, Oxford, 1997.
[24] R. Penrose, Bull. Inst. Math. 10 (1974) 266.
[25] C. Janot, Quasicrystals: A Primer, second ed., Oxford University Press, Oxford, 1994.
[26] L.B. McCusker, R.B. von Dreele, D.E. Cox, D. Louër, P. Scardi, J. Appl. Cryst. 32 (1999) 36.